Structural Engineering and Mechanics, Vol. 31, No. 5 (2009) 587-603
DOI: http://dx.doi.org/10.12989/sem.2009.31.5.587

Free vibration of laminated composite skew plates with central cutouts

Sang-Youl Lee

Industry-Academy Cooperative Foundation, Joongbu University, 101 Daehak-ro, Chungnam 312-702, Korea

Taehyo Park†

Department of Civil Engineering, Hanyang University, 17 Haengdang, Seoul 133-791, Korea

(Received January 8, 2008, Accepted February 26, 2009)

Abstract. We performed a free vibration analysis of skew composite laminates with or without cutout based on the high-order shear deformation plate theory (HSDT). The effects of skew angles and ply orientations on the natural frequencies for various boundary conditions are studied using a nonlinear high-order finite element program developed for this study. The numerical results are in good agreement with those reported by other investigators for simple test cases, and the new results reported in this paper show the interactions between the skew angle, layup sequence and cutout size on the free vibration of the laminate. The findings highlight the importance of skew angles when analyzing laminated composite skew plates with cutout or without cutout.

Keywords: composite laminates; skew plates; finite element analysis; high-order shear deformation plate theory; free vibration; skew angles; cutout ratios.

1. Introduction

Skew plates are often used in modern structures, despite the mathematical difficulties encountered in their analysis. Swept wings of airplanes, for example, can be idealized by introducing substructures in the form of oblique plates. Similarly, complex alignment problems in bridge designs are often solved by using skew plates. Numerous other applications of oblique parallelogram slabs can also be found in buildings. With the advancement in fiber-reinforced composite material technology, the applicability of composites to such skew members has increased greatly due to their low density, high stiffness and high strength. In addition, cutouts are inevitable in structures made of laminated composite materials. Cutouts in structural members may result in a change in the dynamic characteristics for increased skew angles.

The structural behavior of isotropic skew plates without cutout has been studied previously by many investigators using a variety of approaches. Kennedy and Huggins (1964) derived approximate analytical solutions of clamped isotropic oblique plates subjected to uniform lateral

† Professor, Corresponding author, E-mail: cepark@hanyang.ac.kr

load that were subsequently modified and applied to bridge deck designs by Kennedy and Tamberg (1969). Durvasula (1969) presented the natural frequencies of thin skew isotropic plates using the Galerkin method with conventional beam mode function. Mizusawa *et al.* (1979) dealt with natural frequencies of skew isotropic plates using a B-spline Rayleigh-Ritz method. In addition to these analytical approaches, vibration problems using numerical methods have been attempted by many investigators. For example, Bardell (1992) carried out a free vibration analysis of skew plates using a hierarchical finite element method.

All these works are limited in that they analyze only skew plate members made of isotropic materials. Recently, techniques for analyzing laminated composite skew plates made of anisotropic materials have evolved. Wang (1997) examined the free vibration of laminated composite skew plates using a B-spline Rayleigh-Ritz method, which was based on the first-order shear deformation plate theory (FSDT). Anlas and Göker (2001) used orthogonal polynomials with the Ritz method to determine the natural frequencies of skew laminates. Reddy and Palaninathan (1999) introduced a general high-precision triangular plate bending finite element method for a free vibration analysis of laminated skew plates by deriving the consistent mass matrix in explicit form. Wang *et al.* (2000) presented a free vibration analysis of skew sandwich plates with laminated facings. Most of these works were based on classical plate theory (CLPT) or FSDT. In general, a linear FSDT can describe easily and accurately the vibration characteristics of square or rectangular composite plate (Reddy 2004). However, it requires an estimation of shear correction factors; a value of K = 5/6 is normally used (Khdeir and Reddy 1991, Kim and Park 2002). On the other hand, the nonlinear HSDT is free of such requirements and can thus yield more accurate results under both static and dynamic conditions. Many HSDTs exist but they are mostly applicable to rectangular isotropic or anisotropic plates with or without cutout (Murthy 1981, Bhimaraddi and Stevens 1984, Reddy and Phan 1985, Kant *et al.* 1990, Lee and Yhim 2004, Sivakumar and Iyengar 1999, Reddy and Krishnan 2001, Kumar and Shrivastava 2005, Park *et al.* 2008). In this paper, we extend a finite element analysis based on the HSDT to study the free vibration of laminated composite skew plates with cutout. To our knowledge, rare previous reports on this topic exist in the literature; the present paper attempts to fill this gap.

The numerical results are compared to results found in the open literature using simple cases to demonstrate the validity of the approach. For composite skew laminates, the skew angles and layup sequences could play a dominant role in determining the vibration characteristics (Hosokawa *et al.* 1996, Han and Dickinson 1997). Thus, the study is extended to investigate the influence of skew angles and fiber orientations for various boundary conditions. The signicance of the HSDT in analyzing laminated composite skew plates is enunciated in this paper. Then, skew laminates with cutout is presented to explain the complicated effects of the interaction between skew angles and cutout sizes on the free vibration.

2. Theoretical formulation

The HSDT used to analyze composite laminates reviewed in this study is derived from the high-order laminate formulation (Reddy 2004). The theory was based on the same assumptions as those of classical and first-order plate theories, except that we no longer assume that the straight lines normal to the middle surface remain straight after deformation but it is assumed that they can be expressed in the form of a cubic equation. Fig. 1 schematically shows the different deformation

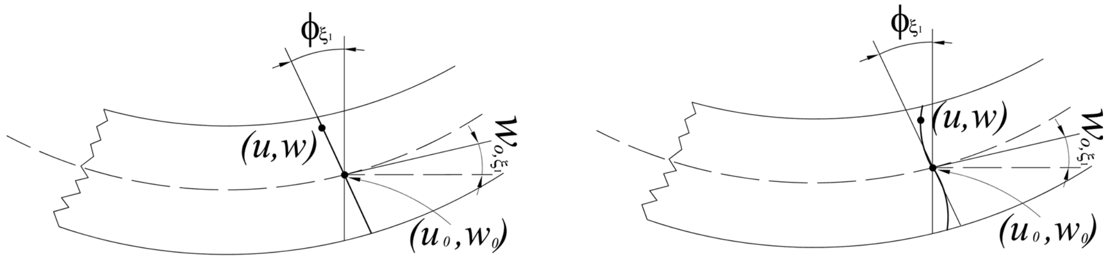

(a) Linear FDST (b) Non-linear HSDT

Fig. 1 Assumed deformation normal to the mid-surface of a plate

kinematics of the FSDT and HSDT. For the FSDT, the following linear relationship with five degrees of freedom per node was used:

$$
\begin{aligned}
u(\xi_1, \xi_2, x_3, t) &= u_0(\xi_1, \xi_2, t) + x_3 \phi_{\xi_1}(\xi_1, \xi_2, t) \\
v(\xi_1, \xi_2, x_3, t) &= v_0(\xi_1, \xi_2, t) + x_3 \phi_{\xi_2}(\xi_1, \xi_2, t) \\
w(\xi_1, \xi_2, x_3, t) &= w_0(\xi_1, \xi_2, t)
\end{aligned}
\tag{1}
$$

For the HSDT, the following non-linear relationship with seven degrees of freedom per node was used

$$
\begin{aligned}
u(\xi_1, \xi_2, x_3, t) &= u_0(\xi_1, \xi_2, t) + x_3 \phi_{\xi_1}(\xi_1, \xi_2, t) - c_1 x_3^3(\phi_{\xi_1} + c_0 w_{0,\xi_1}) \\
v(\xi_1, \xi_2, x_3, t) &= v_0(\xi_1, \xi_2, t) + x_3 \phi_{\xi_2}(\xi_1, \xi_2, t) - c_1 x_3^3(\phi_{\xi_2} + c_0 w_{0,\xi_2}) \\
w(\xi_1, \xi_2, x_3, t) &= w_0(\xi_1, \xi_2, t)
\end{aligned}
\tag{2}
$$

where c_0 and c_1 are the parameters referred to as *tracers*. The condition $c_0 = 1$, $\phi_{\xi_1} = -w_{0,\xi_1}$ and $\phi_{\xi_2} = -w_{0,\xi_2}$ in Eq. (2) yields the same displacement field as that of the classical lamination theory (CLPT). The displacement field becomes identical to that of FSDT for $c_1 = 0$ as shown in Eq. (1). Note that $c_0 = 1$ for HSDT.

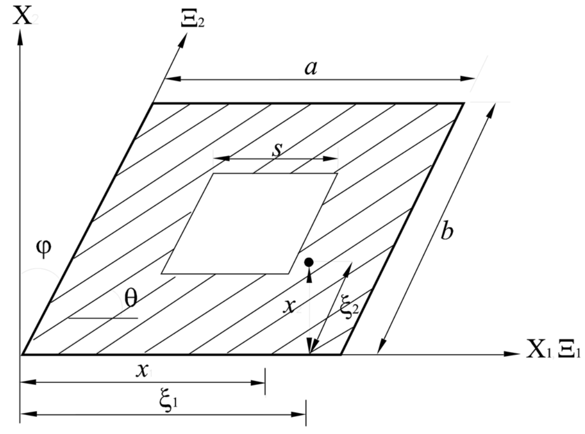

Fig. 2 Geometry of a laminated composite skew plate with cutout

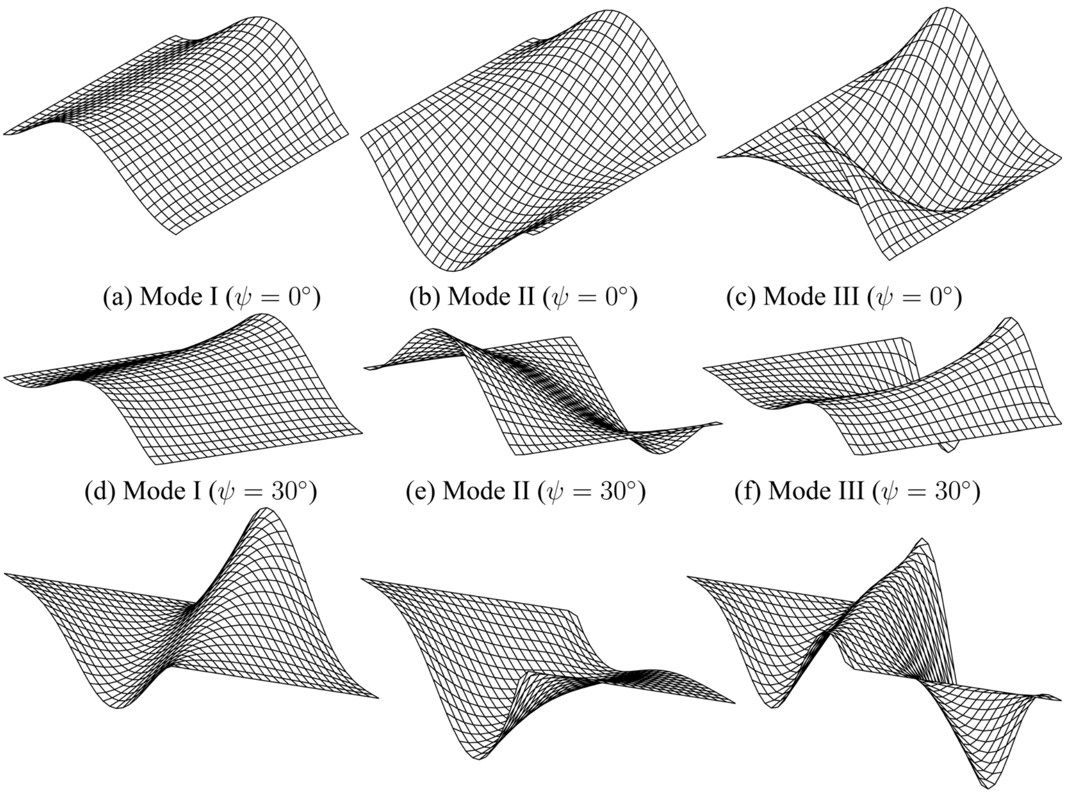

(a) Mode I ($\psi = 0°$) (b) Mode II ($\psi = 0°$) (c) Mode III ($\psi = 0°$)

(d) Mode I ($\psi = 30°$) (e) Mode II ($\psi = 30°$) (f) Mode III ($\psi = 30°$)

(g) Mode I ($\psi = 60°$) (h) Mode II ($\psi = 60°$) (i) Mode III ($\psi = 60°$)

Fig. 3 Mode shapes of the lowest modes for $[45^o/\text{-}45^o]_s$ free-clamped composite skew plates without cutout (a/h = 10.0)

The governing equation of composite skew plates can be obtained conveniently by introducing an oblique coordinate system, as shown in Fig. 2 (Szilard 1974). The coordinates of the rectangular (X_1, X_2, X_3) and oblique (Ξ_1, Ξ_2, Ξ_3) systems are related by

$$\xi_1 = x_1 - x_2 \tan\psi, \quad \xi_2 = \frac{1}{\cos\psi} x_2 \tag{3}$$

The shear deformation theory and the relevant formulas in the finite element analysis of skew plates are reviewed below. A nonconforming element for skew plates have seven degrees of freedom (DOF) per node, that is, the mid-plane displacements in the Ξ_1, Ξ_2, and X_3-directions (u_0, v_0, w_0), the respective derivatives $(w_{0,\xi_1}, w_{0,\xi_2})$, and the rotations $(\phi_{\xi_1}, \phi_{\xi_2})$ are transformed from the rectangular to oblique coordinate system shown in Fig. 3. The generalized displacements can be approximated over an element Ω^e by the expressions

$$\begin{Bmatrix} u_0 \\ v_0 \\ \phi_{\xi_1} \\ \phi_{\xi_2} \end{Bmatrix} = \sum_{j=1}^{4} \Psi_j [I_2] \begin{Bmatrix} u_{0j} \\ v_{0j} \\ \phi_{\xi_{1j}} \\ \phi_{\xi_{2j}} \end{Bmatrix} \quad \text{and} \quad \begin{Bmatrix} w_0 \\ w_{0,\xi_1} \\ w_{0,\xi_2} \end{Bmatrix} = \sum_{j=1}^{4} \begin{bmatrix} \Phi_j & \Phi_j & \Phi_j \\ \Phi_{j,\xi_1} & \Phi_{j,\xi_1} & \Phi_{j,\xi_1} \\ \Phi_{j,\xi_2} & \Phi_{j,\xi_2} & \Phi_{j,\xi_2} \end{bmatrix} \begin{Bmatrix} w_{0j} \\ w_{0j,\xi_1} \\ w_{0j,\xi_2} \end{Bmatrix} \tag{4}$$

where $[I_2]$ is a 2×2 identity matrix, Ψ_j are the Lagrange interpolation functions and Φ_j, Φ_{j,ξ_1} and Φ_{j,ξ_2} are the Hermite interpolation functions, and their first derivatives, respectively.

The stiffness matrix $[K]_e$ of a plate element is assumed to be

$$[K]_e = \int_0^a \int_0^b [B]^T [D_s][B] d\xi_1 d\xi_2 \tag{5}$$

where a and b are the dimensions of a skew plate, $[B]$ is the strain-displacement matrix, and $[D_s]$ is a stiffness matrix in the global coordinates. Alternatively, Eq. (3) can be rewritten in the natural coordinates $(\bar{\xi}_1, \bar{\xi}_2)$ as

$$[K]_r = \int_{-1}^1 \int_{-1}^1 [\bar{B}]^T [D_s][\bar{B}] d\bar{\xi}_1 d\bar{\xi}_2 \tag{6}$$

where $|J|$ is the determinant of Jacobian matrix. The 13×28 strain-displacement matrix $[\bar{B}]$ in the $(\bar{\xi}_1, \bar{\xi}_2)$ coordinates is given by

$$[\bar{B}] = \sum_{j=1}^{4} \begin{bmatrix} \Psi_{j,\bar{\xi}_1} & 0 & 0 & 0 & 0 & 0 & 0 \\ 0 & \Psi_{j,\bar{\xi}_2} & 0 & 0 & 0 & 0 & 0 \\ \Psi_{j,\bar{\xi}_1} & \Psi_{j,\bar{\xi}_2} & 0 & 0 & 0 & 0 & 0 \\ 0 & 0 & 0 & 0 & 0 & \Psi_{j,\bar{\xi}_1} & 0 \\ 0 & 0 & 0 & 0 & 0 & 0 & \Psi_{j,\bar{\xi}_2} \\ 0 & 0 & 0 & 0 & 0 & \Psi_{j,\bar{\xi}_1} & \Psi_{j,\bar{\xi}_2} \\ 0 & 0 & -c_1\Phi_{j,\bar{\xi}_1,\bar{\xi}_1} & -c_1\Phi'_{j,\bar{\xi}_1,\bar{\xi}_1} & -c_1\Phi''_{j,\bar{\xi}_1,\bar{\xi}_1} & -c_1\Psi_{j,\bar{\xi}_1} & 0 \\ 0 & 0 & -c_1\Phi_{j,\bar{\xi}_2,\bar{\xi}_2} & -c_1\Phi'_{j,\bar{\xi}_2,\bar{\xi}_2} & -c_1\Phi''_{j,\bar{\xi}_2,\bar{\xi}_2} & 0 & -c_1\Psi_{j,\bar{\xi}_2} \\ 0 & 0 & -c_1\Phi_{j,\bar{\xi}_1,\bar{\xi}_2} & -c_1\Phi'_{j,\bar{\xi}_1,\bar{\xi}_2} & -c_1\Phi''_{j,\bar{\xi}_1,\bar{\xi}_2} & -c_1\Psi_{j,\bar{\xi}_1} & -c_1\Psi_{j,\bar{\xi}_2} \\ 0 & 0 & \Phi_{j,\bar{\xi}_2} & 0 & 0 & 0 & \Psi_j \\ 0 & 0 & \Phi_{j,\bar{\xi}_1} & 0 & 0 & \Psi_j & 0 \\ 0 & 0 & -c_2\Phi_{j,\bar{\xi}_2} & 0 & 0 & 0 & -c_2\Psi_j \\ 0 & 0 & -c_2\Phi_{j,\bar{\xi}_2} & 0 & 0 & -c_2\Psi_j & 0 \end{bmatrix} \tag{7}$$

and the 13×13 stiffness matrix $[D_s]$ could be expressed as

$$[D_s] = \begin{bmatrix} [A] & [B] & [C] & 0 & 0 \\ [B] & [D] & [F] & 0 & 0 \\ [E] & [F] & [H] & 0 & 0 \\ 0 & 0 & 0 & [A] & [D] \\ 0 & 0 & 0 & [D] & [F] \end{bmatrix} \tag{8}$$

where

$$(A_{ij}, B_{ij}, D_{ij}, E_{ij}, F_{ij}, H_{ij}) = \sum_{k=1}^{n} \int_{x_{3k}}^{x_{3k+1}} \overline{Q}_{ij}^{(k)} (1, x_3, x_3^2, x_3^3, x_3^4, x_3^6) dx_3, \quad i,j = 1,2,6 \tag{9}$$

$$(A_{ij}, D_{ij}, F_{ij}) = \sum_{k=1}^{n} \int_{x_{3k}}^{x_{3k+1}} \overline{Q}_{ij}^{(k)} (1, x_3^2, x_3^6) dx_3, \quad i,j = 4,5 \tag{10}$$

Here, $\overline{Q}_{ij}^{(k)}$ denotes the stiffnesses of the kth layer and the positions of the top and bottom faces of the kth layer $x_{3_{k+1}}$ and x_{3k}.

The equations of motion for the laminated composite skew plate based on the high-order theory can be written as follows

$$N_{\xi_1\xi_1,\xi_1} + N_{\xi_1\xi_2,\xi_2} = I_0\ddot{u}_0 + J_1\ddot{\phi}_{\xi_1} - c_1 I_3 \ddot{w}_{0,\xi_1}$$

$$N_{\xi_1\xi_2,\xi_1} + N_{\xi_2\xi_2,\xi_2} = I_0\ddot{v}_0 + J_1\ddot{\phi}_{\xi_2} - c_1 I_3 \ddot{w}_{0,\xi_2}$$

$$\overline{Q}_{\xi_1,\xi_1} + \overline{Q}_{\xi_2,\xi_2} + c_1(P_{\xi_1\xi_1,\xi_1\xi_1} + 2P_{\xi_1\xi_2,\xi_1\xi_2} + P_{\xi_2\xi_2,\xi_2\xi_2}) + F$$

$$= I_0\ddot{w}_0 - c_1^2 I_6(\ddot{w}_{0,\xi_1\xi_1} + \ddot{w}_{0,\xi_2\xi_2}) + c_1[I_3(\ddot{u}_{0,\xi_1} + \ddot{v}_{0,\xi_2}) + J_4(\ddot{\phi}_{\xi_1,\xi_1} + \ddot{\phi}_{\xi_2,\xi_2})]$$

$$\overline{M}_{\xi_1,\xi_1} + \overline{M}_{\xi_1\xi_2,\xi_2} - \overline{Q}_{\xi_1} = J_1\ddot{u}_0 + K_2\ddot{\phi}_{\xi_1} - c_1 J_4 \ddot{w}_{0,\xi_1}$$

$$\overline{M}_{\xi_1 xi_2,\xi_1} + \overline{M}_{\xi_2\xi_2,\xi_2} - \overline{Q}_{\xi_2} = J_1\ddot{v}_0 + K_2\ddot{\phi}_{\xi_2} - c_1 J_4 \ddot{w}_{0,\xi_2} \tag{11}$$

where $N_{\xi_1\xi_1}, N_{\xi_2\xi_2}$, and $N_{\xi_1\xi_2}$ are the normal and shear force resultants, $\overline{M}_{\xi_1\xi_1}, \overline{M}_{\xi_2\xi_2}$, and $\overline{M}_{\xi_1\xi_2}$ are the moment resultants, $\overline{Q}_{\xi_1}$ and $\overline{Q}_{\xi_2}$ are the transverse force resultants, F is the distributed load, and

$$\overline{M}_{\alpha\beta} = M_{\alpha\beta} - c_1 P_{\alpha\beta}, \quad \overline{Q}_\alpha = Q_\alpha - c_2 R_\alpha \tag{12}$$

$$I_i = \sum_{k=1}^{m} \int_{x_{3k}}^{x_{3k+1}} \rho^{(k)} x_3^i dz \qquad (i = 0, 1, 2, \ldots, 6) \tag{13}$$

$$J_i = I_i - c_1 I_{i+2}, \quad K_2 = I_2 - 2c_1 I_4 + c_1^2 I_6, \quad c_1 = \frac{4}{3h^2}, \quad c_2 = 3c_1 \tag{14}$$

where m is the total number of layers, $\rho^{(k)}$ is the mass density of the kth layer, h is the wall thickness, and $(P_{\xi_1\xi_1}, P_{\xi_2\xi_2}, P_{\xi_1\xi_2})$ and (R_{ξ_1}, R_{ξ_2}) denote the higher-order resultants respectively given as

$$\begin{Bmatrix} P_{\xi_1\xi_1} \\ P_{\xi_2\xi_2} \\ P_{\xi_1\xi_2} \end{Bmatrix} = \int_{-h/2}^{h/2} \begin{Bmatrix} \sigma_{\xi_1\xi_1} \\ \sigma_{\xi_2\xi_2} \\ \sigma_{\xi_1\xi_2} \end{Bmatrix} x_3^3 dx_3, \quad \begin{Bmatrix} R_{\xi_1} \\ R_{\xi_2} \end{Bmatrix} = \int_{-h/2}^{h/2} \begin{Bmatrix} \sigma_{\xi_2 x_3} \\ \sigma_{\xi_1 x_3} \end{Bmatrix} x_3^2 dx_3 \tag{15}$$

Eq. (11) can be rewritten in compact form as

$$\{S\} = [\mu]\{A\} \tag{16}$$

where $\{S\}$, $[\mu]$, and $\{A\}$ are respectively the force vector, inertia matrix, and the acceleration vector. The mass matrix of the skew element is given by the relationship

$$[M]_e = \int_0^a \int_0^b [H]^T [\mu][H] d\xi_1 d\xi_2 = \int_{-1}^{1} \int_{-1}^{1} [\overline{H}]^T [\mu][\overline{H}] |J| d\bar{\xi}_1 d\bar{\xi}_2 \tag{17}$$

where $[\overline{H}]$ is a matrix consisting of Lagrange and Hermite interpolation functions. For a free vibration, the equation of motion is written in the form

$$\{[\overline{M}] - \overline{\omega}^2 [\overline{K}]\} = \{0\} \tag{18}$$

where $[\overline{M}]$ and $[\overline{K}]$ are assembled matrices of $[M]_e$ and $[K]_r$ in the plate. In order to understand the dynamic behavior of a system, we often need to know only a few low order eigenvalues of the system. In this study, the subspace iteration method (Bathe 1996) is adopted to extract the eigenpairs representing the low order natural frequencies. This method selects a subspace whose dimensions, determined by the desired number of eigenvalues to be obtained, are the same as those of the entire matrix. Then, the Jacobi iteration method is carried out on the selected matrix using the Ritz's base vector as an initial vector. This method has the advantages to effective memory management and computational efficiency compared to other methods that carry the entire matrix in the computation (Bathe 1996).

3. Numerical results

This study is focused on the free vibration characteristics of composite skew plates based on the HSDT. The material properties used in the present analysis are listed in Table 1. All the layers were of equal thickness and the skew plates, which were clamped and simply supported on all sides, were considered separately. For a simply supported edge

$$\text{SS-1: } u_0 = v_0 = w_0 = 0 \quad \text{at} \quad \xi_1 = 0, a \text{ and } \xi_2 = 0, b \tag{19}$$

$$\begin{aligned} \text{SS-2: } & v_0 = w_0 = \phi_{\xi 2} = 0 \quad \text{at} \quad \xi_1 = 0, a \\ & u_0 = w_0 = \phi_{\xi 1} = 0 \quad \text{at} \quad \xi_2 = 0, b \end{aligned} \tag{20}$$

For a clamped edge

$$u_0 = v_0 = w_0 = 0, \ \phi_{\xi 1} = 0, \ w_{0,\xi_1} = 0 \text{ and } \xi_1 = 0, a \tag{21}$$

$$u_0 = v_0 = w_0 = 0, \ \phi_{\xi 2} = 0, \ w_{0,\xi_2} = 0 \text{ and } \xi_2 = 0, b \tag{22}$$

Table 1 Mechanical and physical properties of the materials used in this study. The units of E_1, E_2, G_{12}, G_{23}, G_{13} are GPa and that of ρ is kg/m^3, respectively. Note that the properties of Material I and II are normalized by E_2

Material	E_1	E_2	G_{12}	G_{23}	G_{13}	ν_{12}	ν_{21}	ρ
Material I	$40E_2$	-	$0.6E_2$	$0.5E_2$	$0.6E_2$	0.25	0.25	-
Material II	$25E_2$	-	$0.5E_2$	$0.2E_2$	$0.5E_2$	0.25	0.25	-
Material III	130.0	10.0	5.0	3.3	5.0	0.35	0.35	1500.0

Table 2 Normalized frequencies of a square $[0^o/90^o]_2$ antisymmetric cross-ply laminate made of Material I. Letters F, S and C denote free, simply supported (SS-2), and clamped conditions, respectively. $\omega = \bar{\omega} b^2 \sqrt{\rho/E_2}/h$

				Normalized frequency, ω			
Source	b/h	Theory	Solution	F-S	S-S	S-C	C-C
Reddy (2004)	5	HSDT	Exact	6.387	9.087	10.393	11.890
			FEM	6.192	9.103	10.582	12.053
		FSDT	Exact	6.213	8.833	9.822	10.897
			FEM	6.219	8.837	9.899	10.906
		CLPT	Exact	7.450	10.721	13.627	17.741
			FEM	7.279	11.192	15.357	18.694
This study		HSDT	FEM	6.083	9.194	10.435	11.972
Reddy (2004)	10	HSDT	Exact	7.277	10.568	12.870	15.709
			FEM	7.134	10.594	13.180	15.914
		FSDT	Exact	7.215	10.473	12.610	15.152
			FEM	7.222	10.480	12.791	15.181
		CLPT	Exact	7.636	11.154	14.223	18.543
			FEM	7.345	11.383	14.828	19.053
This study		HSDT	FEM	7.489	10.573	12.885	15.745

3.1 Skew plates without cutout

It was shown from our previous study (Lee and Wooh 2004) that the results obtained using different composite plate theories could be significantly different for rectangular or folded plates, depending on the given boundary conditions. In addition, Table 2 shows the effect of the length-to-thickness ratio on the normalized natural frequencies of antisymmetric cross-ply square plates ($[0^o/90^o]_n$, b/h = 5.0, 10.0). The parallel edges on the side of the plate were simply supported (SS-2) and three different boundary conditions were considered for the other two edges of the same plate. As expected, the exact solutions and numerical results obtained from this study are in good agreement with those reported by Reddy (2004). On the other hand, the results obtained using the FSDT and HSDT could be noticeably different depending on the given boundary conditions and length-to-thickness ratio. Difference of about 9.5% for moderately thick plates (b/h = 5.0) with a C-C boundary condition are shown in the table. The differences are much less at lower values of b/h.

Fig. 3 shows the mode shapes of $[45^o/-45^o]_s$ composite skew plates with two clamped and two free edges. The HSDT was used here to obtain better computational accuracy. It is interesting to observe that the first mode shape is antisymmetric for a skew angle of 60^o as shown in Fig. 3(g). This is clearly due to the effect of bending and shear couplings resulting from the increased skew angle. The extent of the effect is determined by the fiber orientation and the length-to-thickness ratio.

Table 3 shows the normalized natural frequencies of $[45^o/-45^o/45^o/-45^o/45^o]$ simply supported square and skew plates made of material I. In this case, the use of different theories make little difference to the composite plate results regardless of the skew conditions, because the length-to-thickness ratio of the plate is relatively low (b/h = 1000.0). On the other hand, for the thicker plate

Table 3 Normalized values of low order natural frequencies for free vibration of five-layered [45°/-45°/45°/-45°/45°] simply supported (SS-1) square and skew plates made of Material I ($\omega = \overline{\omega} b^2/\pi^2 h\sqrt{\rho/E_2}$; a/b = 1 ; a/h = 1000.0)

Skew angle ψ	Mode	Normalized frequency, ω			
		This study (HSDT)	This study (FSDT)	Wang (1997) (FSDT)	Singha and Ganapathi (2004) (FSDT)
0° (Square plate)	1	2.4284	2.4181	2.4339	2.4339
	2	4.9905	4.9678	4.9865	4.9859
	3	6.1367	6.1394	6.1818	6.1814
	4	8.5183	8.4275	8.4870	9.4849
	5	10.2214	10.2528	10.2536	10.2506
	6	11.4669	11.5682	11.6464	11.6433
30° (Skew plate)	1	2.6040	2.5942	2.6119	2.6118
	2	5.6476	5.6622	5.6902	5.6890
	3	6.7934	6.7971	6.8316	6.8308
	4	9.3342	9.3931	9.4773	9.4737
	5	11.7903	11.8545	11.8900	11.8828
	6	13.0764	13.2505	13.2355	13.2258

Table 4 Normalized values of low order natural frequencies for free vibration of five-layered [45°/ -45°/45°/-45°/45°] simply supported (SS-1) and clamped (CCCC) skew plates made of Material I ($\omega = \overline{\omega} b^2/\pi^2 h\sqrt{\rho/E_2}$; a/b = 1 ; a/h = 10.0)

Skew angle ψ	Mode	Normalized frequency, ω			
		SS-1		CCCC	
		This study (HSDT)	Wang (1997) (FSDT)	This study (HSDT)	Wang (1997) (FSDT)
0° (Square plate)	1	1.8431	1.8792	2.3086	2.2857
	2	3.2909	3.3776	3.7482	3.7392
	3	3.6663	3.6924	4.0569	3.9813
	4	4.7888	4.9682	5.1631	5.1800
	5	5.4066	5.4835	5.7649	5.7019
	6	5.5992	5.6002	5.9499	5.8455
30° (Skew plate)	1	2.0605	2.0002	2.6260	2.6626
	2	3.6023	3.6269	4.0636	4.1367
	3	4.1902	4.2830	4.6501	4.7227
	4	4.9952	5.0708	5.4037	5.4950
	5	5.9986	6.2499	6.3307	6.5410
	6	6.4766	6.5351	6.8075	6.8830
45° (Skew plate)	1	2.5238	2.4788	3.2951	3.3523
	2	4.1432	4.2214	4.7067	4.8079
	3	5.4112	5.5857	5.9581	6.0520
	4	5.5012	5.5981	5.9649	6.1029
	5	5.9392	7.0029	7.2176	7.4169
	6	7.4251	7.6255	7.7490	7.9276

Table 5 Normalized natural frequencies of clamped skew plates based in the HSDT for various values of *a/h* ratio (Material II, $[0/90]_s$, $\omega = \overline{\omega} b^2 \sqrt{\rho / E_2} / h$)

		Normalized frequency, ω				
		Length-to-thickness ratio, *a/h*				
Skew angle	Mode	5	10	20	50	100
0°	1	1.1085	1.7809	2.5343	3.1561	3.3050
	2	1.7357	2.8027	3.8452	4.5736	4.7501
	3	1.8752	3.1374	4.9829	7.2149	7.6261
	4	2.3041	3.8166	5.7594	7.2694	7.9530
30°	1	1.2655	2.0425	2.8711	3.5344	3.6950
	2	1.8770	3.1169	4.5075	5.5396	5.7905
	3	2.2155	3.6808	5.5982	7.8540	8.6105
	4	2.4099	4.0603	6.1662	8.2209	8.8382
45°	1	1.5397	2.5373	3.5897	4.3985	4.5976
	2	2.1592	3.6541	5.4945	7.1363	7.5769
	3	2.6928	4.6129	7.1134	9.6004	10.3994
	4	2.7659	4.6816	7.2053	9.9189	10.7934

(*b/h* = 10.0), the difference between the FSDT and HSDT increases with the increased skew angle because of the effect of the high order terms in Eqs. (9) and (10). The natural frequencies of square and skew composite plates with simply supported (SS-1) and clamped edges are compared in Table 4. Table 5 shows the effect of the length-to-thickness ratio on the natural frequency of a four-layered symmetric cross-ply $[0°/90°]_s$ skew laminate with clamped edges. The results obtained from the HSDT are represented in the table.

Fig. 4 shows the natural frequencies of a symmetric and antisymmetric cross-ply composite plate for increasing skew angles. For all clamped boundaries, the induced frequency tends to increase sharply as shown in Fig. 4(a), especially for $\psi > 30°$. The frequencies for antisymmetric laminates are higher than those for symmetric laminates, but the difference between FSDT and HSDT results is negligible. In contrast, the frequencies show different trends for the cantilever (Fig. 4(b)). The difference between the FSDT and HSDT results increases to a maximum difference of about 14% and the induced frequencies for the antisymmetric case are much higher than those for the symmetric case, especially for $\psi < 30°$. This is predictable because it is expected that a free edge without restraints is normally susceptible to vibration effects when skew angles and layup sequences are combined. The difference becomes more dramatic for the case with simple (SS-1)-free edges shown in Fig. 5. For the all clamped edges, the natural frequencies increase at a constant rate with the fiber angle, and the difference between the FSDT and HSDT results increases for both $\psi = 30°$ and 60° (Fig. 5(a)). On the other hand, for simple-free edges, the natural frequencies exhibit their highest values within the range of fiber angles from 40° to 50° (Fig. 5(b)). In addition, it can be observed that the difference between the FSDT and HSDT results for free edges is much greater than that of all clamped edges. We may conclude from these results that the natural frequency of a composite plate with a free edge is significantly influenced by the skew and fiber angles. Therefore, we must carefully consider the high-order shear terms in the HSDT, which are heavily dependent on other factors such as the shape and boundary conditions as well as the fiber orientation.

Fig. 6 shows the frequency of a clamped antisymmetric cross-ply skew plate for an increasing

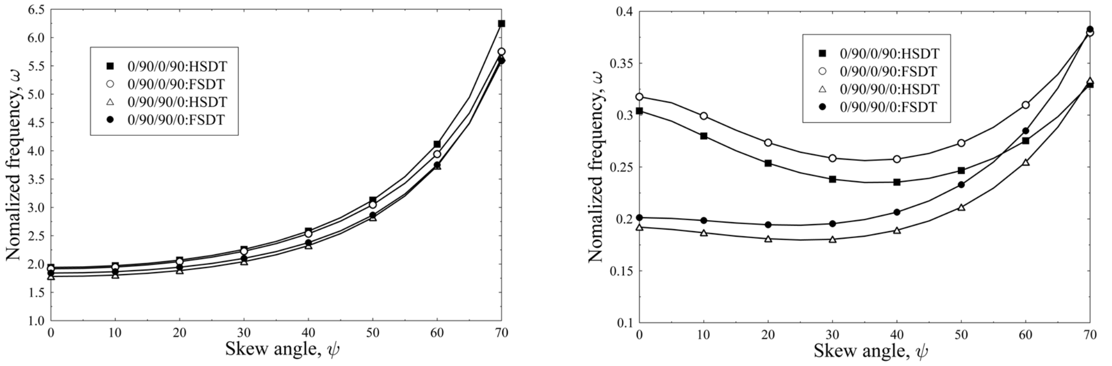

(a) All clamped edges

(b) Cantilever

Fig. 4 First-order natural frequency of symmetric and antisymmetric cross-ply composite plates for increased skew angles (Material II, a/h = 10.0, $\omega = \overline{\omega}b^2/h\sqrt{\rho/E_2}$)

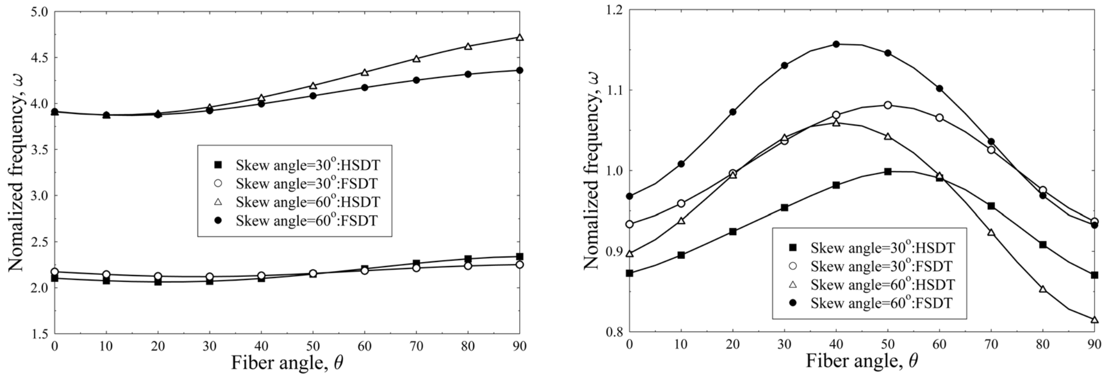

(a) All clamped edges

(b) Two simple (SS-1) and two free edges

Fig. 5 First-order natural frequency of [90°/θ°/θ°/90°] composite skew plates for increased fiber angles (Material II, a/h = 10.0, $\omega = \overline{\omega}b^2/h\sqrt{\rho/E_2}$)

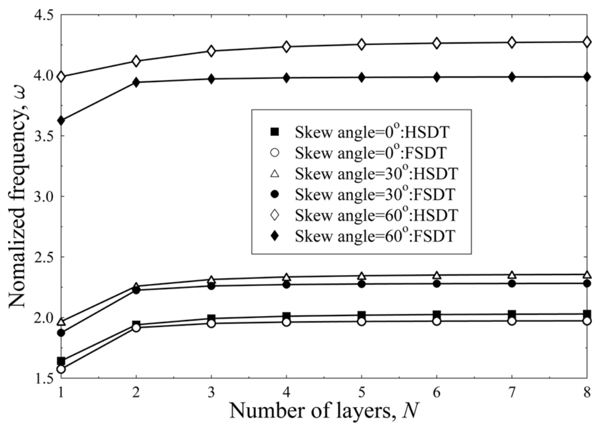

Fig. 6 First-order natural frequency of clamped $[0°/90°]_N$ composite skew plates for increased number of layers (Material II, a/h = 10.0, $\omega = \overline{\omega}b^2/h\sqrt{\rho/E_2}$)

number of layers. The values in the figure approach a constant, regardless of the skew angle, as the number of layers increases, especially for $N > 3$. As shown in the figure, the rate of convergence of the FSDT and HSDT results shows similar trends, but the frequency amplitude of the laminate with $\psi = 60^o$ is significantly greater than that of the others. Furthermore, a larger difference is observed between the FSDT and HSDT results for $\psi = 60^o$. This is probably due to the different dynamic characteristics of a plate with $\psi = 60^o$ as illustrated in Fig. 3. The high-order shear terms in the HSDT for the large skew angle of $\psi = 60^o$ are signified by the transformation of the material coefficients (see Eqs. (9) and (10)) in oblique coordinates. The coupling stiffness B_{ij} and E_{ij} in Eq. (9), which become nonzero for antisymmetric laminates, is more influenced by the frequencies of the plate with the increased skew angle. Therefore, we may not neglect the shear terms when analyzing composite skew plate structures because the contributions made by the high-order terms could be substantial.

3.2 Skew plates with cutout

Table 6 shows the effect of the cutout size on the normalized natural frequencies of simply supported square plates made of Material III ($[(\pm45^o/0^o_2)_3(90^o/0_2^o/90^o)_2]_s$, b/h = 75). The square cutout ratio is varied from 0.0 to 0.6 in step of 0.2. It can be observed from the table that the results obtained from this study are in good agreement with those reported by Kumar and Shrivastava (2005) and commercial package model (ABAQUS 6.7, 2007). For all clamped boundaries, the comparison of results in Table 7 also shows that the present results are in close agreement with those of Kumar and Shrivastava (2005) and ABAQUS. The frequencies for the 0.2 and 0.4 cutout

Table 6 Normalized values of low order natural frequencies for free vibration of forty-layered $[(\pm45^o/0^o_2)_3(90^o/0^o_2/90^o)_2]_s$ simply supported (SS-1) square plates with cutout ($\omega = \bar{\omega} b^2/h\sqrt{\rho/E_2}$; a/h = 75 ; Material III)

Cutout ratio (s/b)	Mode	Normalized frequency, ω			
		This study (HSDT)	Kumar and Shrivastava (2005) (HSDT)	Kumar and Shrivastava (2005) (FSDT)	ABAQUS (FSDT)
0.0	1	13.592	13.714	13.590	13.685
	2	29.003	29.503	29.113	29.894
	3	37.665	38.309	37.792	39.103
	4	53.607	54.852	53.934	55.568
0.2	1	13.113	13.403	13.154	13.162
	2	28.245	29.061	28.391	29.213
	3	35.527	36.903	35.790	37.154
	4	51.961	53.421	52.401	53.881
0.4	1	14.173	14.862	14.243	14.222
	2	25.642	26.683	25.651	26.212
	3	28.603	29.912	28.640	29.389
	4	48.260	49.765	48.719	50.182
0.6	1	19.338	21.064	19.527	19.421
	2	27.812	30.061	28.204	28.205
	3	28.865	31.418	29.376	29.321
	4	43.980	49.424	45.223	45.881

Table 7 Normalized values of low order natural frequencies for free vibration of forty-layered $[(\pm 45^o/0^o{}_2)_3(90^o/0^o{}_2/90^o)_2]_s$ clamped square plates with cutout ($\omega = \bar{\omega} b^2/h\sqrt{\rho/E_2}$; a/h = 15 ; Material III)

Cutout ratio (s/b)	Mode	Normalized frequency, ω This study (HSDT)	Kumar and Shrivastava (2005) (HSDT)	ABAQUS (FSDT)
0.2	1	21.031	21.501	20.853
	2	32.464	32.893	32.957
	3	36.980	37.834	37.340
	4	50.744	50.477	50.602
0.4	1	26.922	27.522	26.902
	2	31.851	32.067	31.307
	3	35.510	35.986	34.975
	4	47.208	47.910	47.522
0.6	1	43.287	45.488	44.040
	2	47.311	45.720	44.142
	3	55.765	54.905	52.647
	4	60.054	57.770	55.113

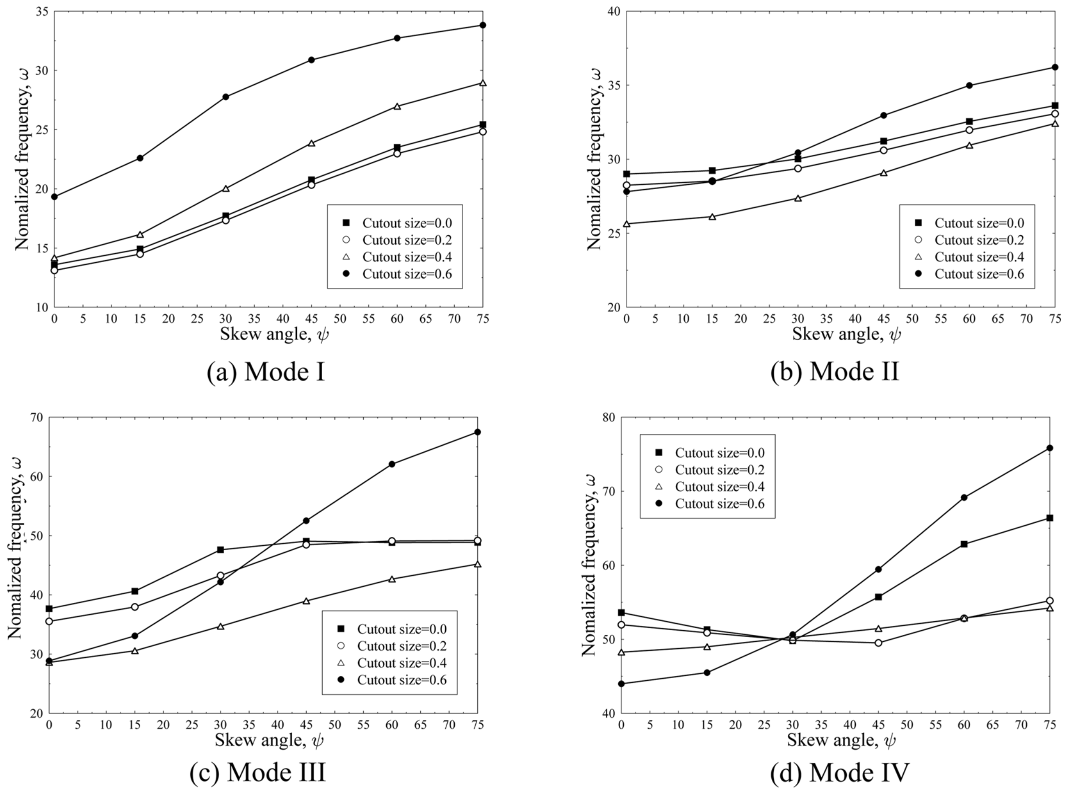

(a) Mode I

(b) Mode II

(c) Mode III

(d) Mode IV

Fig. 7 Normalized values of low order natural frequencies for free vibration of forty-layered $[(\pm 45^o/0^o{}_2)_3(90^o/0^o{}_2/90^o)_2]_s$ simply supported (SS-1) square and skew plates with cutout ($\omega = \bar{\omega} b^2/h\sqrt{\rho/E_2}$; a/h = 75 ; Material III) ratios are closed to that of the plate without cutout. On the other hand, the induced frequency for the cutout ratio of 0.6 is extremely higher than the others. This is predictable because it is expected that the plate mass decreases as the cutout ratio increases. We can also notice that the frequency is significantly altered for the 0.6 cutout ratio regardless of the boundary condition.

Fig. 7 shows the natural frequencies of a forty-layered simply supported composite plate with different cutout ratios for increasing skew angles. As the skew angle increases, the differences in frequencies due to different skew angles are small for a great number of layers as shown in Fig. 6. On the other hand, for the large cutout size (s/b > 0.2), the differences when compared to those of square plates increase, especially for skew angles of ψ = 30° and 45°. This implies that there is signicant change in dynamic characteristics of the skew plate with the large cutout size. The key observations from the figure are various effects of the interaction between skew angles and cutout sizes on the free vibration of plates. Table 8 shows normalized values of low order natural frequencies for free vibration of forty-layered $[(\pm45^o/0_2^o)_3(90^o/0_2^o/90^o)_2]_s$ simply supported (SS-1) square and skew plates with cutout for various values of a/h ratio. The size of the cutout is fixed

Table 8 Normalized values of low order natural frequencies for free vibration of forty-layered $[(\pm45^o/0^o_2)_3(90^o/0^o_2/90^o)_2]_s$ simply supported (SS-1) square and skew plates with cutout for various values of a/h ratio ($\omega = \bar{\omega}b^2/h\sqrt{\rho/E_2}$; s/b = 0.4 ; Material III)

		Normalized frequency, ω				
		Length-to-thickness ratio, a/h				
Skew angle	Mode	5	10	20	40	80
0°	1	10.645	12.829	13.723	14.051	14.170
	2	14.567	19.945	23.412	25.016	25.681
	3	14.955	20.974	25.339	27.629	28.671
	4	20.561	33.326	43.314	47.084	48.330
15°	1	10.685	13.025	14.191	15.044	16.320
	2	14.490	19.835	23.385	25.156	26.225
	3	15.015	21.168	25.752	28.550	30.795
	4	21.049	33.153	42.742	47.129	49.162
30°	1	10.887	13.633	15.517	17.495	20.350
	2	14.452	19.681	23.455	25.684	27.560
	3	15.208	21.695	26.934	30.924	35.149
	4	21.099	32.786	42.083	47.219	50.580
45°	1	11.217	14.573	17.357	20.445	24.236
	2	14.530	19.701	23.835	26.680	29.341
	3	15.538	22.475	28.551	33.854	39.549
	4	20.609	32.176	41.583	47.429	51.873
60°	1	11.577	15.583	19.207	23.135	27.350
	2	14.722	19.911	24.484	27.940	31.259
	3	15.928	23.319	30.234	36.644	43.309
	4	20.509	31.756	41.473	47.989	53.393
75°	1	11.867	16.353	20.547	24.960	29.346
	2	14.932	20.181	25.065	29.023	32.759
	3	16.258	23.979	31.504	38.650	45.879
	4	20.519	31.594	41.584	48.679	54.803

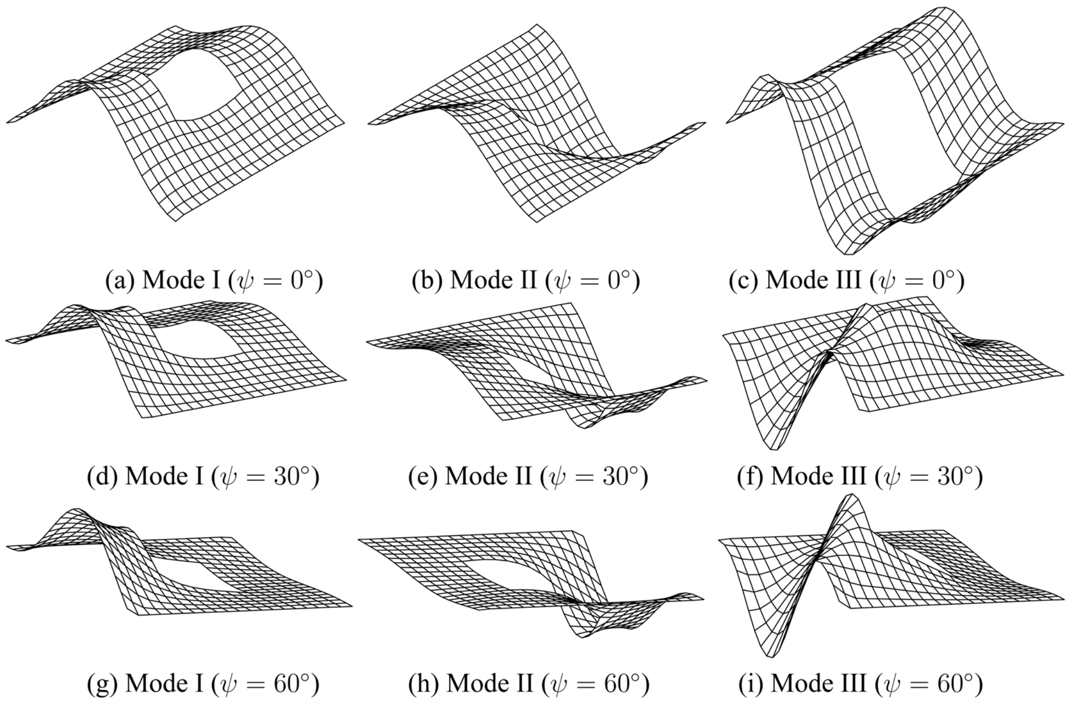

Fig. 8 Mode shapes of the lowest modes for $[45°/\text{-}45°]_s$ free-clamped composite skew plates with cutout (s/b = 0.4, a/h = 10.0)

as s/b = 0.4. It can be observed that the frequency increases as the length-to-thickness ratio. Furthermore, the difference becomes more dramatic as the skew angle increases. Note that the frequency in this case is heavily dependent on the skew angle.

Fig. 8 shows the mode shapes of $[45°/\text{-}45°]_s$ composite skew plates with the central cutout ratio of 0.4. The geometrical and material properties of the skew plate are same as those of Fig. 3. It is interesting to observe that the mode shapes of the plate with cutout are significantly different from those of the plate without cutout, especially for the bigger skew angle. This is clearly due to the interaction effect of resulting from the increased skew angle and cutout ratio. The extent of the dynamic characteristics changed from the effect is determined by the fiber orientation, the length-to-thickness ratio and boundary condition.

4. Conclusions

We developed a technique based on nonlinear high-order plate theory to analyze the free vibration behavior of skew composite structures with or without cutout, which is an attractive approach because it not only is computationally efficient and accurate but it also avoids assumptions about shear factors that are mandatory in a FSDT. The accuracy of the present formulation is demonstrated for rectangular and skew laminates using FSDT and HSDT calculations. The technique is then implemented for rectangular and skew plate structures with various skew angles, cutout ratios, length-to-thickness ratios, layup sequences, and boundary conditions to compare the results obtained from the two different theories.

The use of different plate theories make little difference for thin plates regardless of the skew angles. The difference, however, becomes significant for thick composites, even rectangular ones, depending on the layup configuration and boundary conditions. For skew composites with free edges, the difference is even greater because both the properties of the materials and the geometrical properties of the member have large contributions to the overall behavior of the structure. In specific, skew angles of more than 60^o is very sensitive to the fiber angles and number of layers. In this case, the difference between FSDT and HSDT results increases, especially with the number of layers. Therefore, it is desirable to use a HSDT for better accuracy. The nonlinear effect of through-thickness shear deformations, which largely govern the free vibrations of skew composite structures, should not be neglected for these types of problems. The results of plates with cutout implies that there is significant change in dynamic characteristics of the skew plate with the large cutout size, especially for various length-to thickness ratios. The key observations are various effects of the interaction between skew angles and cutout sizes on the free vibration of plates. The parameter case results of this study may serve as a benchmark for other designers and researchers analyzing free vibrations of laminated composite skew plate structures with or without cutout.

References

ABAQUS (2007), *ABAQUS/CAE User's Manual*, Version 6.7, Hibbitt, Karlsson and Sorensen Inc., USA.

Anlas, G. and Göoker, G. (2001), "Vibration analysis of skew fibre-reinforced composite laminated plates", *J. Sound Vib.*, **242**, 265-276.

Bardell, N.S. (1992), "The free vibration of skew plates using the hierarchical finite element method", *Comput. Struct.*, **45**, 841-874.

Bathe, K.J. (1996), "The finite element procedures in engineering analysis", Prentice Hall, New Jersey.

Bhimaraddi, A. and Stevens, L.K. (1984), "A high order theory for free vibration of orthotropic, homogeneous and laminated rectangular plates", *J. Appl. Mech.*, **51**, 195-198.

Han, W. and Dickinson, S.M. (1997), "Free vibration of symmetrically laminated skew plates", *J. Sound Vib.*, **208**, 367-390.

Hosokawa, K., Terada, Y. and Sakata, T. (1996), "Free vibrations of clamped symmetrically laminated skew plates", *J. Sound Vib.*, **189**, 525-533.

Kant, T., Varaiya, J.H. and Arora, C.P. (1990), "Finite element transient analysis of composite and sandwich plates based on a refined theory and implicit time integration schemes", *Comput. Struct.*, **36**, 401-420.

Kennedy, J.B. and Huggins, M.V. (1964), "Series solution of skewed stiffened plates", *Proc. ASCE*, *J. Eng. Mech. Div.*, **90**, 1-22.

Kennedy, J.B. and Tamberg, K.G. (1969), "Programs of skew in concrete bridge design", Department of Highways, Downsview, Ontario, Canada, Report No. RR144.

Khdeir, A.A. and Reddy, J.N. (1991), "Analytical solutions of refined plate theories of cross-ply composite laminates", *J. Pressure Vessel Tech.*, **113**, 570-578.

Kim, K.D. and Park, T. (2002), "An 8-node assumed strain element with explicit integration for isotropic and laminated composite shells", *Struct. Eng. Mech.*, **13**, 387-410.

Kumar, A. and Shrivastava, R.P. (2005), "Free vibration of square laminates with delamination around a central cutout using HSDT", *Comput. Struct.*, **70**, 317-333.

Lee, S.Y. and Wooh, S.C. (2004), "Finite element vibration analysis of composite box structures using the high order plate theory", *J. Sound Vib.*, **277**, 801-814.

Lee, S.Y. and Yhim, S.S. (2004), "Dynamic analysis of composite plates subjected to multi-moving loads based on a third order theory", *Int. J. Solids Struct.*, **41**, 4457-4472.

Mizusawa, T., Kajita, T. and Naruoka, M. (1979), "Vibration of skew plates by using b-spline function", *J.*

Sound Vib., **62**, 301-308.
Murthy, M.V.V. (1981), “An improved transverse shear deformation theory for laminated anisotropic plates”, NASA Technical Paper. **1903**, 1-37.
Park, T., Lee, S.Y., Seo, J.W. and Voyiadjis, G.Z. (2008), “Structural dynamic behavior of skew sandwich plates with laminated composite faces”, *Compos. Part B*, **39**, 316-326.
Reddy, A.R.K. and Palaninathan, R. (1999), “Free vibration of skew laminates”, *Comput. Struct.*, **70**, 415-423.
Reddy, J.N. (2004), “Mechanics of laminated composite plates and shells : Theory and analysis”, CRC press, New York.
Reddy, J.N. and Phan, N.D. (1985), “Stability and vibration of isotropic, orthotropic, and laminated plates according to a higher-order shear deformation theory”, *J. Sound Vib.*, **98**, 157-170.
Reddy, J.N. and Krishnan, S. (2001), “Vibration control of laminated plates using embedded smart layers”, *Struct. Eng. Mech.*, **12**, 135-156.
Singha, M.K. and Ganapathi, M. (2004), “Large amplitude free flexural vibrations of laminated composite skew plates”, *Int. J. Non-linear Mech.*, **38**, 1709-1720.
Sivakumar, K., Iyengar, N.G.R. and Deb, K. (1999), “Free vibrations of laminated composite plates with cutout”, *J. Sound Vib.*, **221**, 443-470.
Szilard, R. (1974), “Theory and analysis of plates : Classical and numerical methods”, Prentice-hall, New Jersey.
Wang, C.M., Ang, K.K., Yang, L. and Watanabe, E. (2000), “Free vibration of skew sandwich plates with laminated facings”, *J. Sound Vib.*, **235**, 317-340.
Wang, S. (1997), “Free vibration analysis of skew fibre-reinforced composite laminates based on first-order shear deformation plate theory”, *Comput. Struct.*, **63**, 525-538.